Electronic Supplementary Material (ESI) for Journal of Materials Chemistry A.
This journal is © The Royal Society of Chemistry 2018

Electronic Supplementary Information for

Improved Capacity of Redox-Active Functional Carbon Cathode by Dimension Reduction for Hybrid Supercapacitors

Tianyuan Liu,[a‡] Byeongyong Lee, [a‡] Michael J. Lee,[a] Jinho Park,[a] Zhongming Chen,[b] Suguru Noda[b] and Seung Woo Lee[a]*

[a] George W. Woodruff School of Mechanical Engineering, Georgia Institute of Technology, Atlanta, Georgia 30332, USA. E-mail: seung.lee@me.gatech.edu

[b] Department of Applied Chemistry, Waseda University, Tokyo 169-8555, Japan.

[‡] These authors contributed equally.

* Corresponding author

Experimental

Material Preparation

Preparation of TDFCs Graphene oxide (GO) was synthesized by the Modified Hummer's method. To prepare the two-dimensional functional carbon sheets (TDFC-X), D-(+)-Glucose (Sigma Aldrich) of 3 mg mL^{-1} was mixed with GO of 0.X mg mL^{-1} (X= 1 or 5) in deionized (DI) water by short sonication for 10 min. The glucose solution with the GO templates was then sealed in a Teflon-lined autoclave for the template-assisted hydrothermal carbonization at 200 °C for 18 h. After the autoclave was naturally cooled down to room temperature, carbonaceous products (TDFC-X) were collected by filtration. Carbon spheres (CSs) were also synthesized by the same process to the TDFC without GO.

Preparation of a Si-based anode The Si-based anode was prepared by hydrothermal assembly of Si nanoparticle and GO. In brief, Si nanoparticles (US Research Nanomaterials, Inc, 50-70 nm) were dispersed in DI water (10 mg mL^{-1} of Si nanoparticle dispersion) and then, 0.1 mL of Poly (diallyldimethylammonium chloride) was added into the Si nanoparticle dispersion to convert

change the surface charge from negative to positive. 3 mL of the Si nanoparticle dispersion was added into 30 mL of 2 mg mL^{-1} GO dispersion. The mixture of the Si nanoparticle and GO was hydrothermally assembled at 180 ^{o}C for 12 h. After the hydrothermal reaction, the obtained hydrogel (Si/RGO) was freeze-dried subsequent thermal annealing at 450 ^{o}C for 3.5 h under Ar environment.

Material characterization

The microstructures of the carbonaceous products and composite films were characterized using a scanning electron microscope (SEM) (Hitachi SU8010, operated at 5 kV), a transmission electron microscope (TEM) (Hitachi HT7700, operated at 120 kV), and atomic force microscopy (AFM) (Veeco AFM). The Raman spectra of carbon materials were collected by a Thermo Nicolet Almega XR Dispersive Raman Spectrometer using a 488-nm wavelength laser. Fourier transform infrared (FTIR) spectra were measured by Thermo Scientific Nicolet iS50 at attenuated total reflectance (ATR) mode. X-ray photoelectron spectroscopy (XPS, Thermal Scientific K-alpha XPS instrument) was employed to analyze the chemical composition of the carbon materials. High-resolution C 1s peaks were fitted using XPSPEAKS 4.1 software. Electrical conductivities of the films were measured by a standard four-point probe configuration (Signatone). Thermogravimetric analysis (TGA) of carbon materials was carried out by Q600 TGA/DSC in a temperature range of 50~700°C under air environment with a ramping rate of 5°C min^{-1}.

Electrochemical measurement

TDFC-X or CS were mixed with few-walled carbon nanotubes (CNTs, 30 wt%) [1] by a sonication. Then vacuum-filtration was performed to prepare free-standing TDFC-X and CS electrodes. In this structure, the CNTs serve as internal current collectors to enable electron transport to the carbonaceous products. The films were dried in a vacuum oven at 70 °C overnight before use. The densities of electrodes were 0.30~0.4 g cm^{-3}. Loading densities of the prepared electrodes were 2.7~9.3 mg cm^{-2} based on the mass of the carbonaceous products. Two-electrode type Swagelok cells were used for electrochemical measurements. Both Li- and Na-cells were assembled in an Argon-filled glovebox (MBraun). The free-standing TDFC (or CS) electrode and a piece of Li (or Na) were used as cathode and anode, respectively. The separators for Li-cells are two pieces of Celgard 2500, while a piece of glass fiber membrane (Whatman) was used for Na-cells. 1 M $LiPF_6$ in a mixture of ethylene carbonate (EC) and dimethyl carbonate (DMC) (3:7 volume ratio, BASF) was used as an electrolyte for Li-cells and 1 M $NaPF_6$ in EC:DMC (3:7 volume ratio) was used as

electrolyte in Na-cells. The voltage window was kept at 1.5-4.5 V vs. Li for Li-cells and 1.3-4.2 V vs. Na for Na-cells, respectively. Current densities were controlled from 0.05 to 5 A/g during the rate-dependent galvanostatic charge/discharge (GCD) tests. At each end of charging and discharging, the voltage was held for 30 min at either 4.5 V or 1.5 V vs. Li for Li-cells (4.2 V or 1.3 V vs. Na for Na-cells). The cycling stability of the carbon electrodes was tested *via* an accelerated cycling method up to 10,000 cycles based on previous reports.[2, 3] The measurement current density was 0.1 A g^{-1} and cycling current density was 10A g^{-1}. Capacitance and capacity in half-cells were normalized by the mass of carbonaceous products (TDFC-X or CS). Electrochemical impedance spectroscopy measurement was performed in the frequency range of 10 mHz-100 kHz with a voltage amplitude of 10 mV. For the full-cell assembly, the Si anode was prepared by mixing 82 wt% of the Si/RGO with super P carbon black as a conductive additive and sodium carboxylic cellulose as a binder. The Si/graphene electrode was assembled with a piece of Li metal and then, pre-lithiated to 0.03 V vs. Li in 1M $LiPF_6$ in EC:DMC with 10% fluoroethylene carbonate (FEC) additive. The lithiated Si electrodes were employed as counter electrodes for TDFC-1 electrodes. The active material mass ratio of anode to cathode was 1:2.4. The Ragone plot of the full-cell was calculated based on the total mass of cathode and anode.

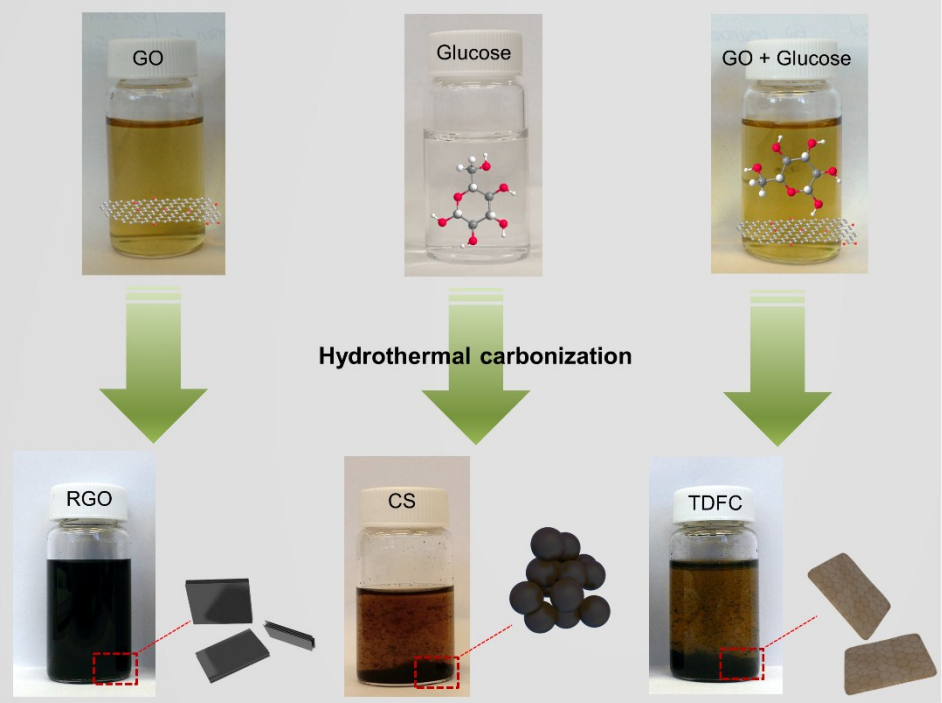

Fig. S1 Digital images before and after the hydrothermal carbonization process. Before the hydrothermal reaction, GO (0.1 mg mL^{-1}, top left), glucose (3 mg mL^{-1}, top middle), and the mixture of GO and glucose (top right) displayed transparent colors. After the hydrothermal reaction, GO, glucose and the mixture were converted into reduced graphene oxide (RGO, bottom left), carbon sphere (CS, bottom middle) and TDFC (bottom right), respectively. RGO showed an opaque dark color. CS and TDFC displayed dark colored precipitates.

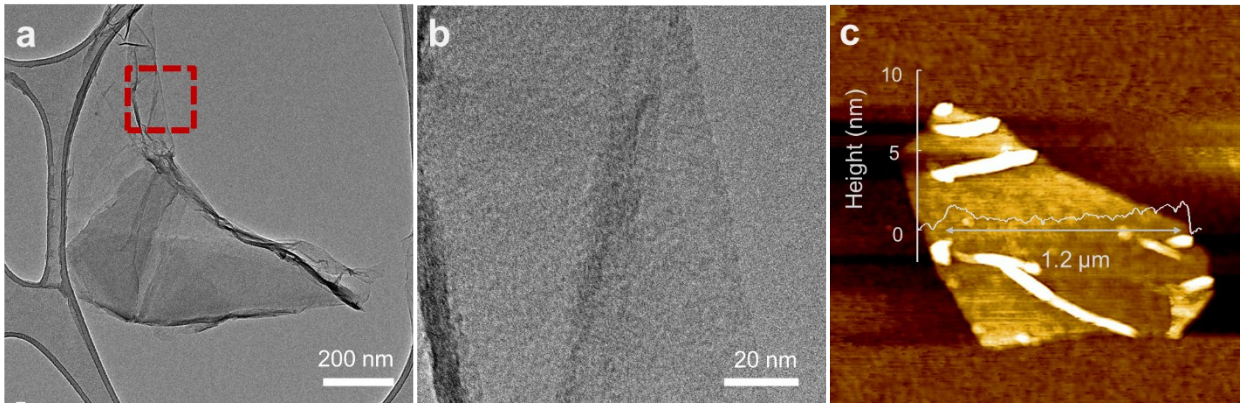

Fig. S2 Morphology characterization of graphene oxide (GO). Transmission electron microscope (TEM) images of GO at (a) low and (b) high magnification. (c) Atomic force spectroscopy (AFM) image of GO. GO shows planar morphology and thin thickness of ~2 nm.

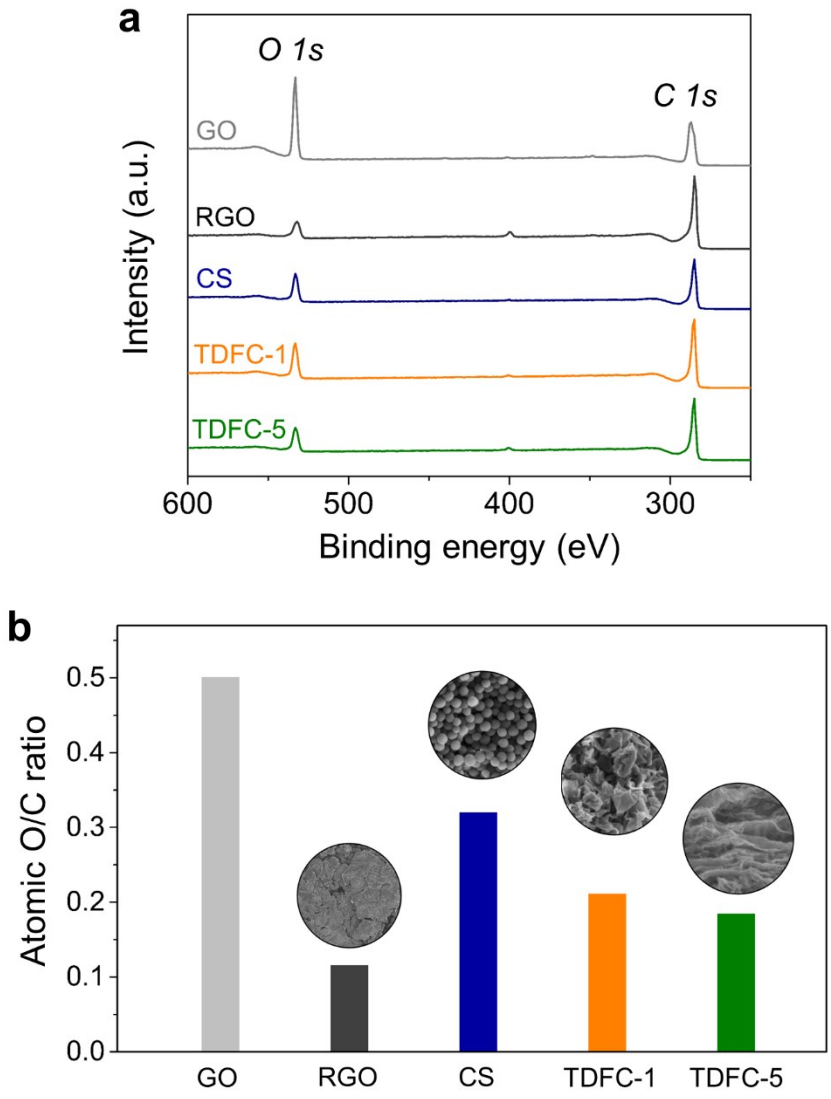

Fig. S3 X-ray photoelectron spectroscopy (XPS) characterization of TDFCs and CS. (a) Wide scan surveys and (b) atomic O/C ratios of the carbonaceous products. As the GO concentration increased from 0 (CS) to 0.5 mg/mL (TDFC-5), the O/C ratio decreased from 0.32 to 0.18.

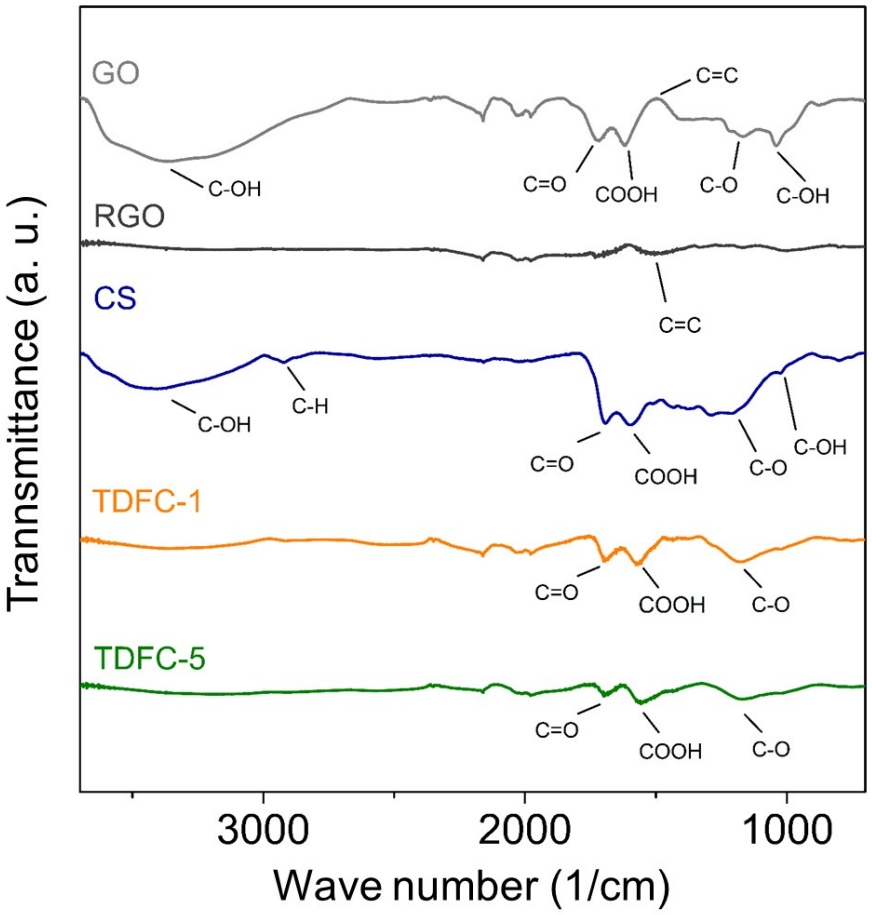

Fig. S4 Fourier transform infrared (FT-IR) spectra of the various carbonaceous products. FTIR spectra of the carbonaceous products shows various oxygen functional groups of -OH (3000-3700, 1020 cm^{-1}), -C=O (1710 cm^{-1}) and -COOH (1620 cm^{-1}). While CS shows clear –OH band peak at 3400 cm^{-1}, TDFCs display a reduced peak intensity for -OH (3000-3700 cm^{-1}).

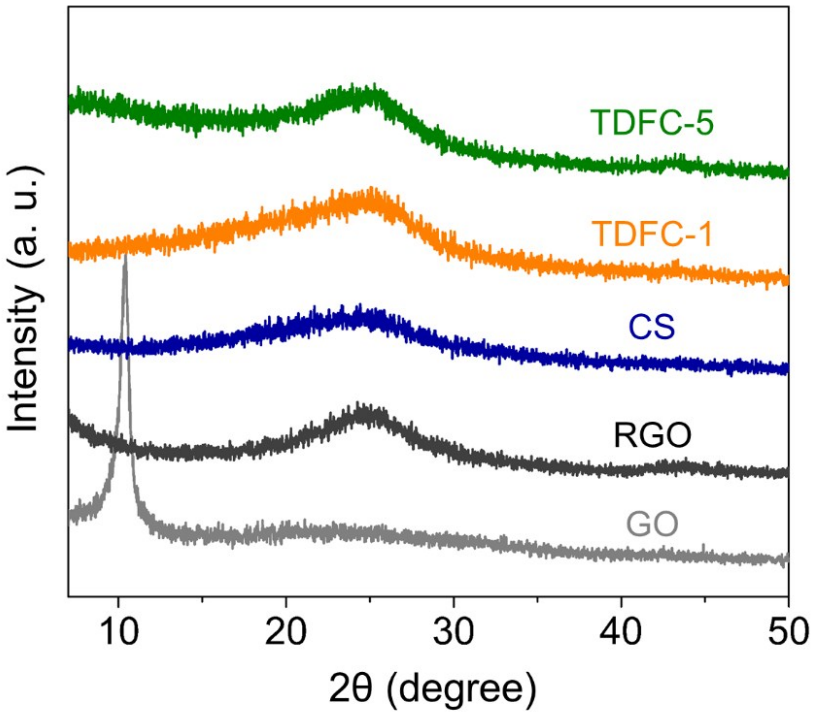

Fig. S5 X-ray diffraction (XRD) investigation of the carbonaceous products. XRD pattern of the GO powder shows a sharp peak at 10.4° and the peak was shifted to 25° after the hydrothermal reduction. TDFCs and CS show broad peaks 25°, but XRD patterns of TDFCs is slightly sharper than that of CS due to the incorporated RGO.

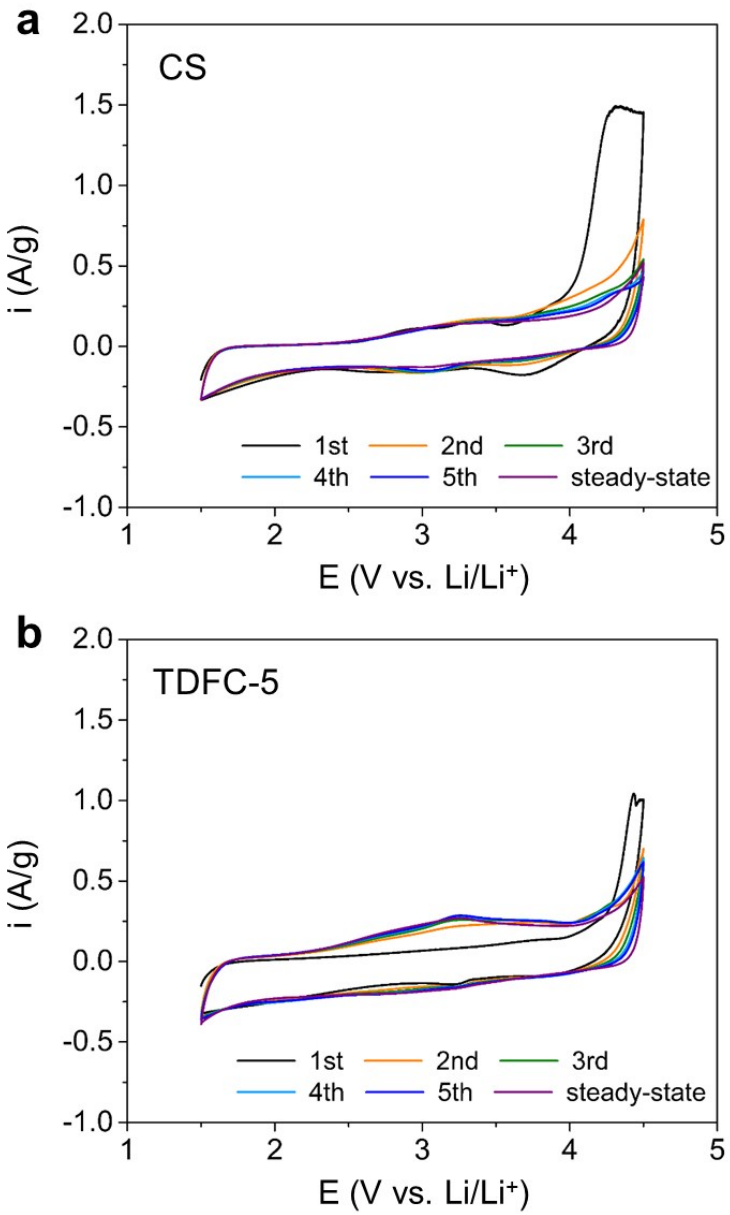

Fig. S6 Electrochemical characterization of CS and TDFC-5 by cyclic voltammetry (CV) scans in Li-cells. Initial and steady-state CV scans of (a) CS and (b) TDFC-5 at 1 mV s^{-1} in Li-cells. CV scans were carried out in the voltage range of 1.5-4.5 V vs. Li/Li^+.

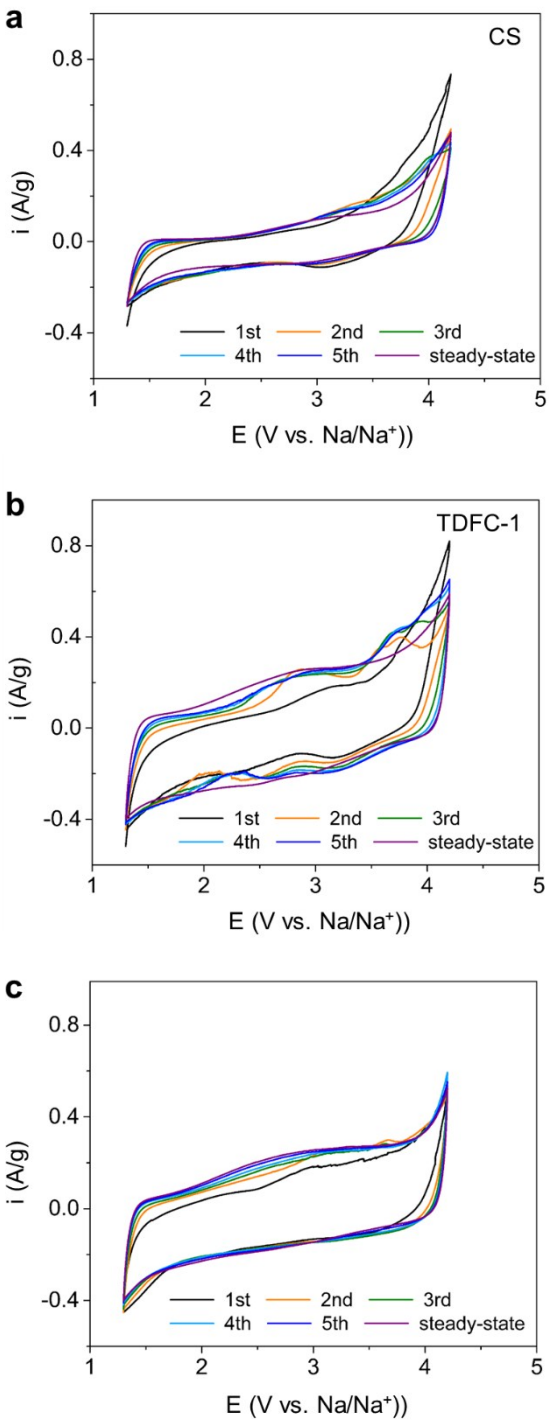

Fig. S7 Electrochemical characterizations of the CS and TDFCs by cyclic voltammetry (CV) scans in Na-cells. Initial and steady-state CV scans of (a) CS, (b) TDFC-1 and (c) TDFC-5 at 1 mV s^{-1} in Na-cells. CV scans were carried out in the voltage range of 1.3-4.2 V vs. Na/Na^+.

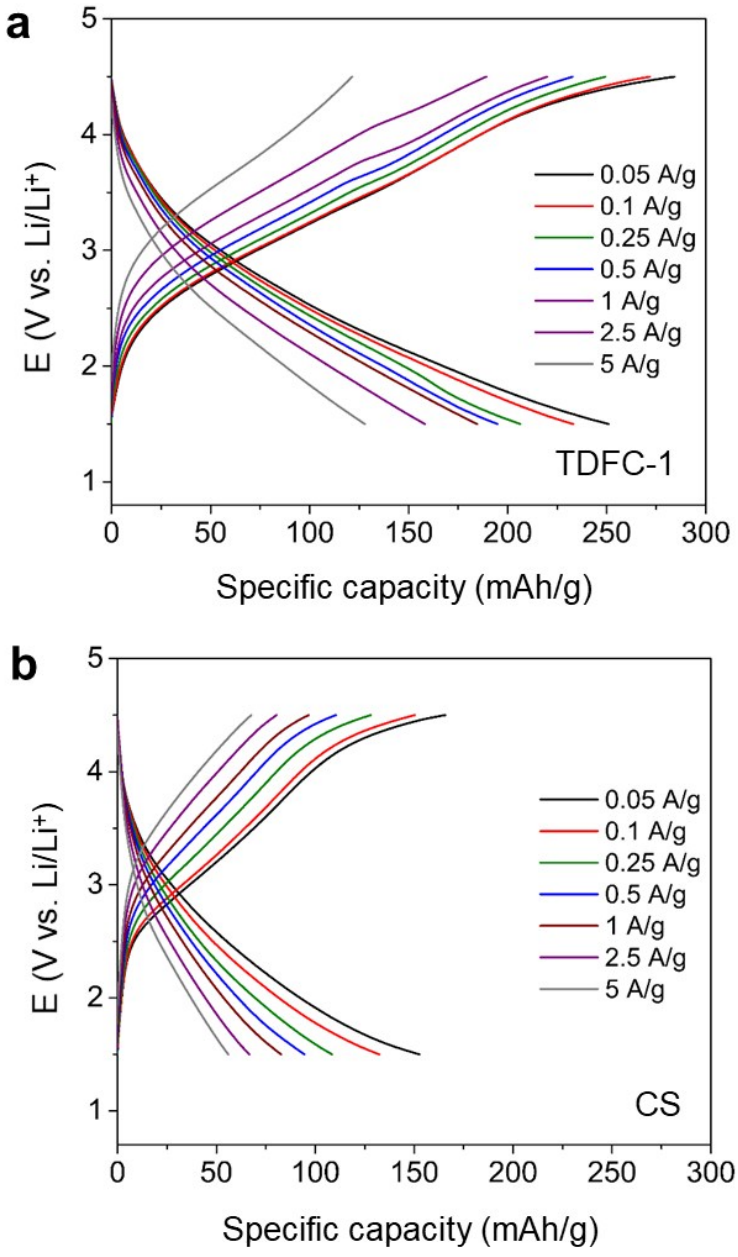

Fig. S8 Rate-dependent galvanostatic charge/discharge (GCD) profiles of TDFC-1 and CS in Li-cells. (a) TDFC-1. (b) CS. Li- -cells were operated in the voltage range of 1.5-4.5 V vs. Li/Li^+. The voltage profiles were measured from 0.05 to 5 A g^{-1}.

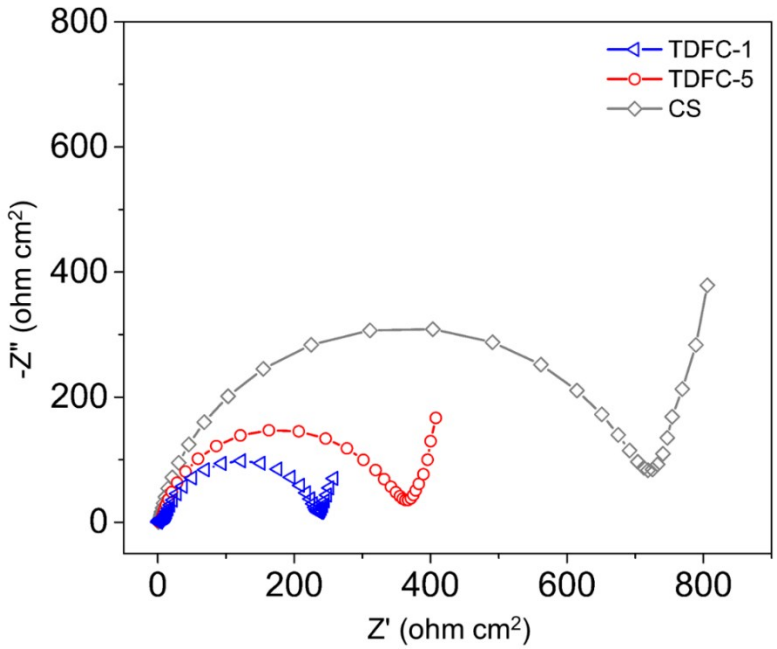

Fig. S9. Electrochemical impedance spectroscopy (EIS) measurement of the carbonaceous products. EIS measurement of TDFC-1, TDFC-5 and CS was carried out from 100 kHz to 10 mHz with an amplitude of 10 mV. The impedance was multiplied by the electrode area to obtain normalized real and imaginary impedances.

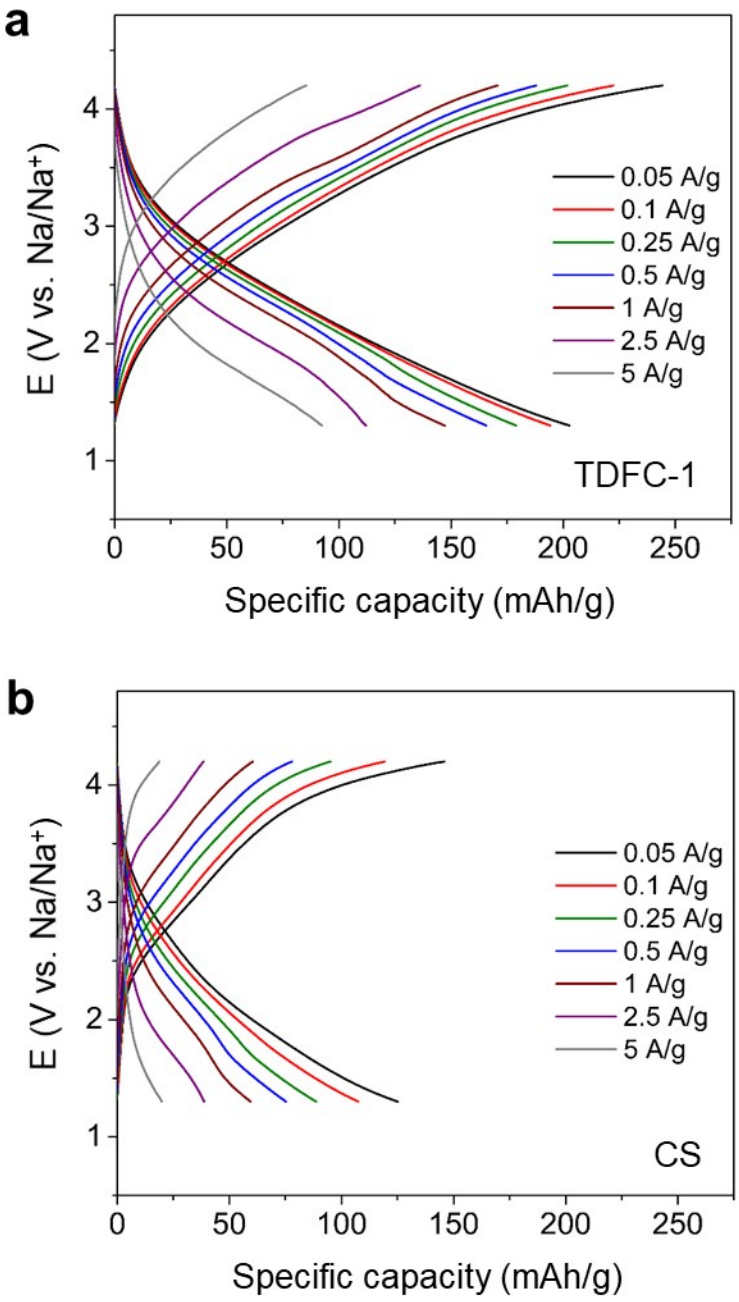

Fig. S10 Rate-dependent galvanostatic charge/discharge (GCD) profiles of TDFC-1 and CS in Na-cells. (a) TDFC-1. (b) CS. Na-cells were operated in the voltage range of 1.3-4.2 V Na/Na^+. The voltage profiles were measured from 0.05 to 5 A g^{-1}.

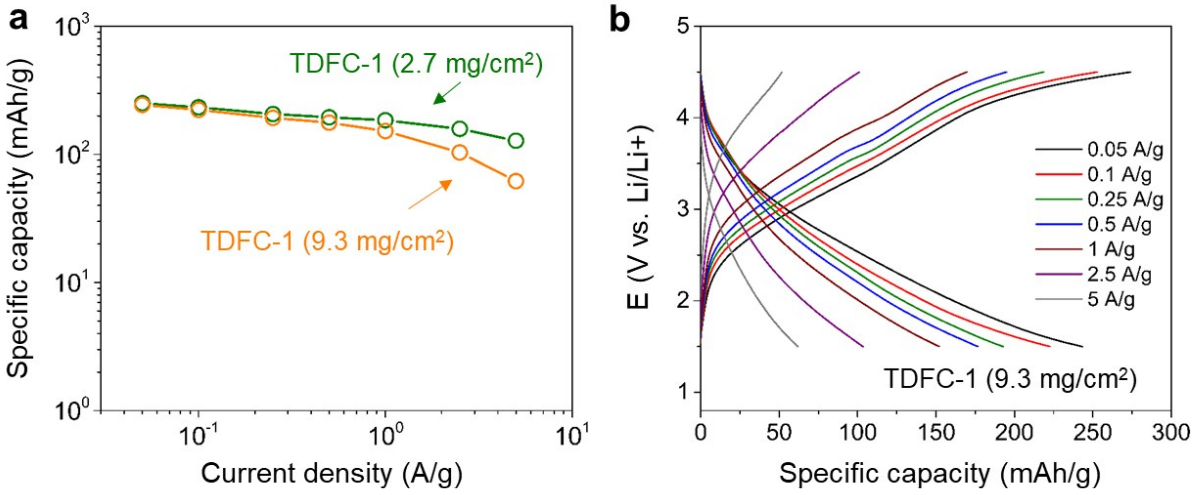

Fig. S11 Rate-dependent capability of TDFC-1 at a high mass loading of 9.3 mg cm^{-2} in Li-cells (a) Comparison of specific discharge capacity of TDFC-1 at different loading scales. (b) Rate-dependent galvanostatic charge/discharge (GCD) profiles of TDFC-1 at the high mass loading (9.3 mg cm^{-2}). Li-cells were operated in the voltage range of 1.5-4.5 V vs. Li at varied current density from 0.05 to 5 A g^{-1}.

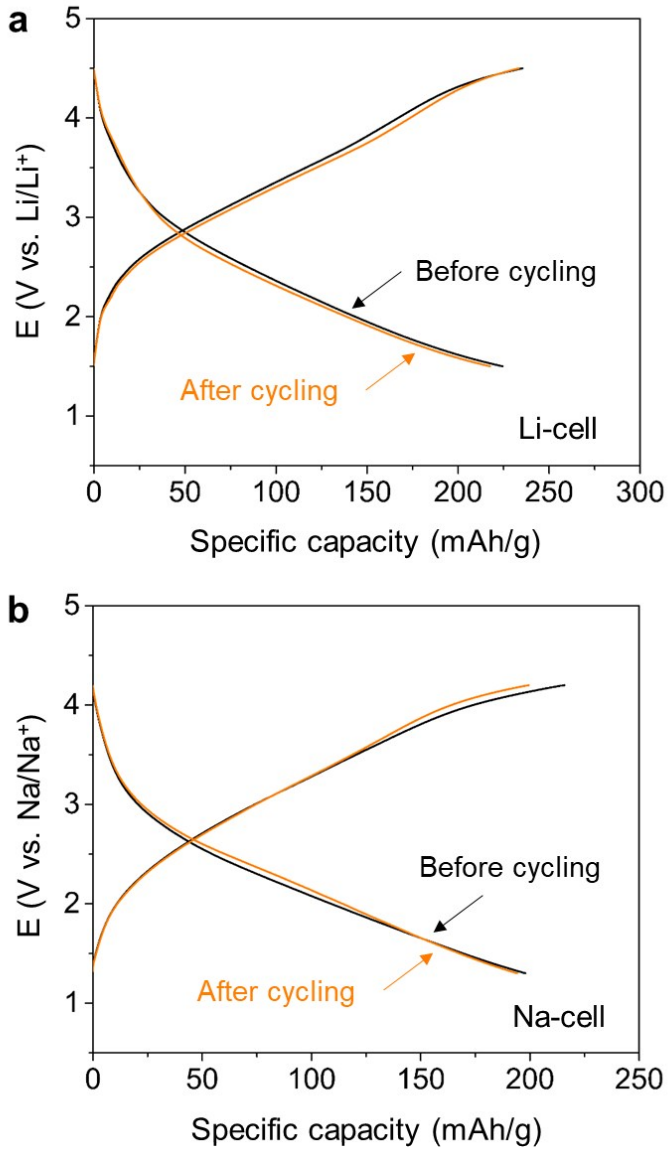

Fig. S12 Charge/discharge profiles of the TDFC-1 before and after cycling. (a) Li-cell at a voltage window of 1.5-4.5 V vs. Li/Li^+. (b) Na-cell at a voltage window of 1.3-4.2 V vs. Na/Na^+. The charge/discharge profiles were measured at a current density of 0.1 A g^{-1}.

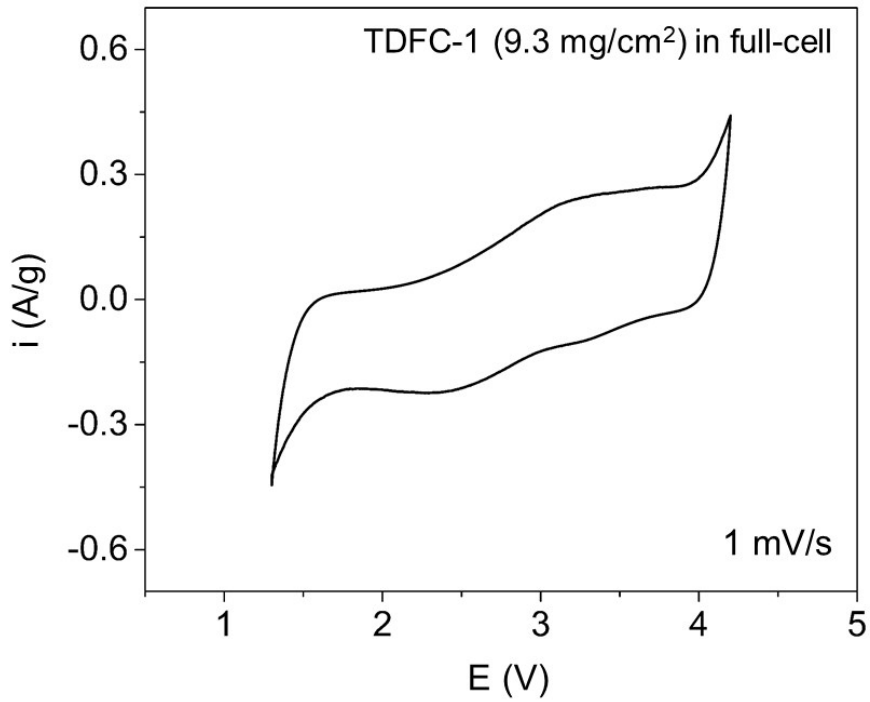

Fig. S13 Cyclic voltammetry (CV) scan of TDFC-1 in a full-cell assembly with a Si-based anode.

For the full-cell assembly, a Si-based anode (Si/RGO) was employed. The full-cell was operated at a voltage window of 1.3-4.2 V with a scan rate of 1mV s^{-1}.

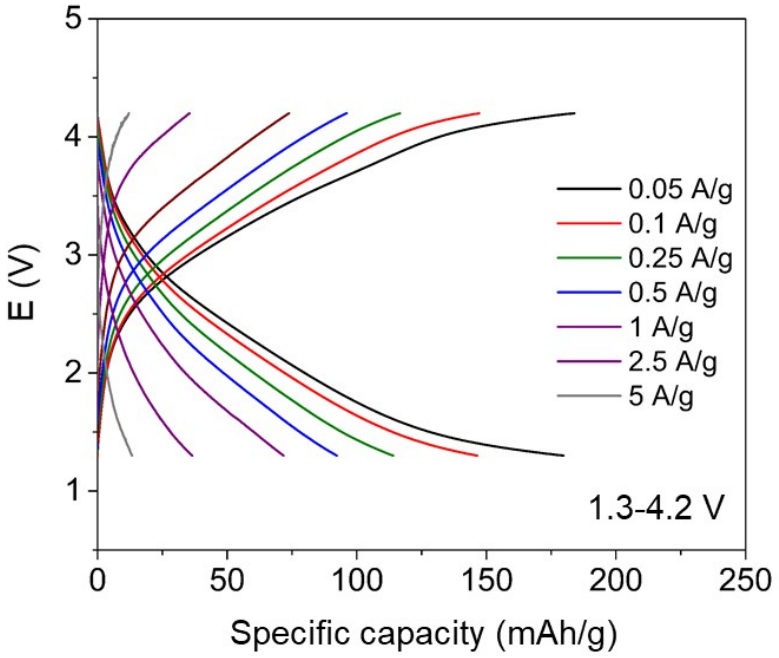

Fig. S14 Rate-dependent galvanostatic charge/discharge (GCD) profiles of TDFC-1 in the full-cell. The full-cell were operated in the voltage range of 1.3-4.2 V at varied current density from 0.05 to 5 A g^{-1}.

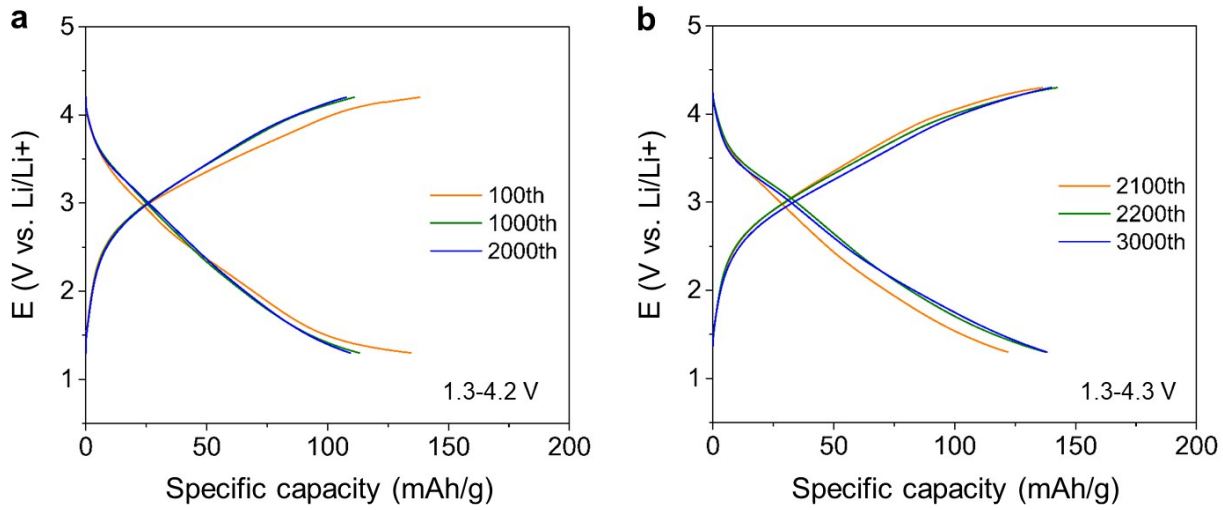

Fig. S15 Charge/discharge voltage profiles of the high mass loading TDFC-1 in a full-cell assembly at various cycles. Voltage profiles of TDFC-1 in a full-cell assembly at various cycles in the voltage range of (a) 1.3-4.2 V and (b) 1.3-4.3 V. The full-cell was cycled in 1.3-4.2 V for 2,000 cycles and then, further cycled in 1.3-4.3 V up to 3,000 cycles.

Table S1. Comparison of gravimetric electrochemical performance of various electrodes.

Material	Loading density (mg/cm^2)	Capacity (mAh/g)	Cycling stability		
			Capacity (mAh/g)	Cycles	Capacity retention
Activated carbon [4]	2	~130 at 0.4A/g (Li)	110	1000	92%
Nitrogen-doped activated carbon [5]	—	130~165 at 0.4 A/g (Na)	110	500	86%
Peanut shell nanosheet carbon [6]	0.4	~165 at 0.1 A/g (Na)	<100	5000	82%
Disodium Rhodizonate [7]	2	~175 at 0. 1A/g (Li)	110	1500	88.2%
$Na_2C_6O_6$ [8]	~0.8	~190 at 0.025 A/g (Na)	<185	100	90%
Poly (benzoquinonyl sulfide) [9]	1~2	~247 at 0.1 A/g (Li) — (Na)	212 180	1000 100	86% 68%
3,4,9,10-perylene-tetracarboxylicacid-dianhydride [10]	2	~130 at 0.02 A/g (Na)	100	200	—
Cuprous 7,7,8,8-tetracyanoquinodimethane [11]	0.9~1.2	~214 at 0.05 A/g (Na)	~205	50	—
$Na_4C_8H_2O_6$ [12]	0.75~1.5	~183 at 0.019 A/g (Na)	154	100	84%
perylene 3,4,9,10-tetracarboxylic dianhydride-based PI [13]	—	137 at 0.05 A/g (Na)	111	5000	87.5%
This work	**2.7~9.3**	**250 at 0.04A/g (Li)** **210 at 0.04A/g (Na)**	**217** **187**	**10000** **10000**	**93%** **94%**

Table S2. Comparison of areal electrochemical performance of various electrodes.

Material	Loading density (mg/cm^2)	Capacity (mAh/cm^2)	Cycling stability		
			Capacity (mAh/cm^2)	Cycles	Capacity retention
Activated carbon [4]	2	~ 0.260 at 0.8 $\mu A/cm^2$ (Li)	0.22	1000	92%
Peanut shell nanosheet carbon [6]	0.4	~ 0.066 at 0.04 $\mu A/cm^2$ (Na)	~0.04	5000	82%
Disodium Rhodizonate [7]	2	0.350 at 0.2 $\mu A/cm^2$ (Li)	0.22	1500	88.2%
$Na_2C_6O_6$ [8]	~0.8	0.152 at 0.02 $\mu A/cm^2$ (Na	~0.15	100	90%
Poly (benzoquinonyl sulfide) [9]	1~2	0.494 at ~0.2 $\mu A/cm^2$ (Li)	0.42	1000	86%
3,4,9,10-perylene-tetracarboxylicacid-dianhydride [10]	2	0.260 at 0.04 $\mu A/cm^2$ (Na)	0.2	200	—
Cuprous 7,7,8,8-tetracyanoquinodimethane [11]	0.9~1.2	0.257 at ~0.06 $\mu A/cm^2$ (Na)	~0.25	50	—
$Na_4C_8H_2O_6$ [12]	0.75~1.5	0.275 at 0.0285 $\mu A/cm^2$ (Na)	~0.23	100	84%
This work	**2.7~9.3**	**2.28 at 0.372 $\mu A/cm^2$ (Li)** **0.567 at 0.108 $\mu A/cm^2$ (Na)**	**2.02** **0.51**	**10000** **10000**	**93%** **94%**

Areal capacity was calculated from the loading-density and gravimetric capacity in table S1.

References

1. K. Hasegawa and S. Noda, *J. Power Sources*, 2016, **321**, 155-162.
2. T. Liu, K. C. Kim, B. Lee, Z. M. Chen, S. Noda, S. S. Jang and S. W. Lee, *Energy Environ. Sci.*, 2017, **10**, 205-215.
3. S. W. Lee, N. Yabuuchi, B. M. Gallant, S. Chen, B. S. Kim, P. T. Hammond and Y. Shao-Horn, *Nat. Nanotechnol.*, 2010, **5**, 531-537.
4. B. Li, F. Dai, Q. F. Xiao, L. Yang, J. M. Shen, C. M. Zhang and M. Cai, *Adv. Energy Mater.*, 2016, **6**., 1600802.
5. B. Li, F. Dai, Q. F. Xiao, L. Yang, J. M. Shen, C. M. Zhang and M. Cai, *Energy Environ. Sci.*, 2016, **9**, 102-106.
6. J. Ding, H. L. Wang, Z. Li, K. Cui, D. Karpuzov, X. H. Tan, A. Kohandehghan and D. Mitlin, *Energy Environ. Sci.*, 2015, **8**, 941-955.
7. C. L. Wang, Y. G. Fang, Y. Xu, L. Y. Liang, M. Zhou, H. P. Zhao and Y. Lei, *Adv. Funct. Mater.*, 2016, **26**, 1777-1786.
8. Y. Q. Wang, Y. Ding, L. J. Pan, Y. Shi, Z. H. Yue, Y. Shi and G. H. Yu, *Nano Lett.*, 2016, **16**, 3329-3334.
9. Z. P. Song, Y. M. Qian, T. Zhang, M. Otani and H. S. Zhou, *Adv. Sci.*, 2015, **2**., 1500124.
10. W. Luo, M. Allen, V. Raju and X. L. Ji, *Adv. Energy Mater.*, 2014, **4**., 1400554.
11. C. Fang, Y. Huang, L. X. Yuan, Y. J. Liu, W. L. Chen, Y. Y. Huang, K. Y. Chen, J. T. Han, Q. J. Liu and Y. H. Huang, *Angew. Chem. Int. Ed.*, 2017, **56**, 6793-6797.
12. S. W. Wang, L. J. Wang, Z. Q. Zhu, Z. Hu, Q. Zhao and J. Chen, *Angew. Chem. Int. Ed.*, 2014, **53**, 5892-5896.
13. H. G. Wang, S. Yuan, D. L. Ma, X. L. Huang, F. L. Meng and X. B. Zhang, *Adv. Energy Mater.*, 2014, **4**., 1301651.